Effects of horizontal transverse isotropy on determination of the orientation of buried geophones

Peter Gagliardi and Don C. Lawton

ABSTRACT

The effects of horizontal transverse isotropy (HTI) on geophone orientation calibration were examined, under the assumption of weak anisotropy. It was found that values of the Thomsen parameters δ and ε as low as ±0.05 could produce deviations in geophone orientation calculations of as much as 5°; it was also found that the maximum deviation in this angle was more sensitive to ε than δ. A model was created using $\varepsilon = 0.1$ and $\delta = 0.025$, which resulted in a maximum polarization angle deviation of 6.45°. Using this model, values for apparent polarization deviation were found for various source locations; these values, when plotted as a function of source-receiver offset, produced distinct trends depending on the orientation of the source-well line. Further investigation of these deviations revealed that they asymptotically approached a particular value as offset increased, due to the behaviour of the source-receiver azimuths. When geophone orientation angle deviations were plotted as a function of source-receiver azimuth, it was found that all lines followed the same trend, regardless of their orientation. The results of this study show that HTI media should be taken into consideration when undertaking orientation calibration for buried microseismic arrays or geophones used in vertical seismic profiles.

INTRODUCTION

Determination of geophone orientation azimuth is an important step for passive seismic monitoring using a borehole geophone array. When a tool is placed into the hole, it has the tendency to spin; however, the proper location of events using these tools requires that we know their orientation. In order to determine their orientation, a controlled experiment is generally performed, using known source locations. When calibrating these geophone orientation angles, there are three helpful assumptions that can be made to greatly simplify the orientation analysis:

1. The well is vertical, ensuring that the horizontal components of the geophone are in the X-Y plane.

2. Strata are horizontal, ensuring that Snell's Law does not cause any lateral raybending.

3. All layers are isotropic, ensuring that the angle measured at the geophone, the phase angle, is equal to the angle pointing back to the source, the group angle. A simple schematic illustrating this difference is shown in Figure 1.

The first of these points is addressed in a paper by Gagliardi and Lawton (2011); it can be overcome by performing a transformation of source coordinates onto a plane defined by the horizontal components of the geophone. The second and third of these have the potential to skew results of a calibration, and continue to introduce error in the locations

of microseismic events that are being monitored. The focus of this paper will be to examine the effects of anisotropy on geophone orientation calibration; this could depend on several factors, such as the type of anisotropy, the strength of anisotropy, and the orientation of the well with respect to the directionality of the anisotropy. In this study, the investigation will be limited to the effects of a single HTI medium on a vertical well.

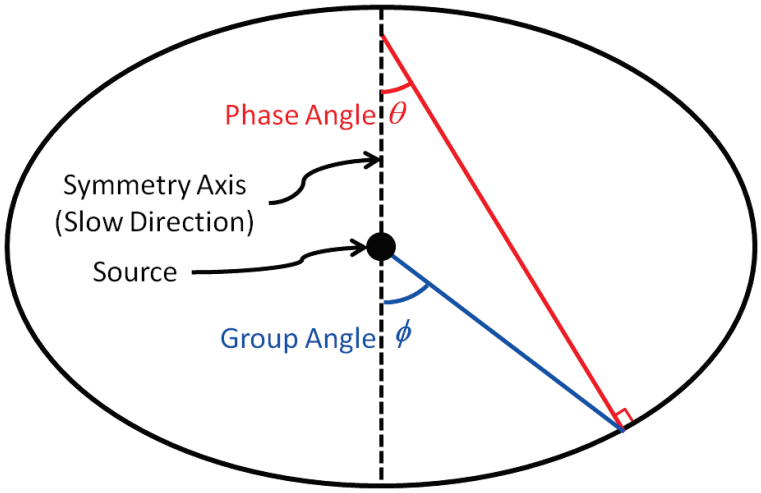

FIG. 1. Simple schematic showing the difference between group angle ϕ and phase angle θ.

THEORY

In the case of weak anisotropy, the phase velocity of a P-wave is given by (Thomsen, 1986)

$$v(\theta) = v_0\{1 + \delta \sin^2\theta \cos^2\theta + \varepsilon \sin^4\theta\}, \quad (1)$$

where v_0 is the velocity parallel to the axis of symmetry, θ is the phase angle, and δ and ε are weak anisotropic parameters, defined in Thomsen (1986). It should be noted that the case of $\delta = \varepsilon$ will result in a special case called elliptical anisotropy (Thomsen, 1986). The group angle can then be calculated using (Vestrum et al., 1999)

$$\phi = \theta + \arctan\left(\frac{\partial v}{\partial \theta}/v\right), \quad (2)$$

where

$$\frac{\partial v}{\partial \theta} = v_0\{2\delta(\cos^3\theta \sin\theta - \cos\theta \sin^3\theta) + 4\varepsilon \cos\theta \sin^3\theta\}. \quad (3)$$

Note that, in a purely HTI medium with a vertical well, ϕ will be the source azimuth with respect to the well, while θ will relate to the direction of polarisation measured by the receiver in the well. Using Equation 2 we can write that the difference between group and phase angle is given by

$$\phi - \theta = \varphi = \arctan\left(\frac{\partial v}{\partial \theta}/v\right); \quad (4)$$

this will contribute to deviation in geophone orientation calibration. The following analytic examples are meant to give a sense of the magnitude of deviation involved.

ANALYTIC EXAMPLES

Maximum angle difference dependent on δ and ε

Using Equation 4, the maximum angle difference can be computed for a range of values of δ and ε. Figure 2 shows a contour plot of these values, given on a range of $-0.15 \leq \delta \leq 0.15$, $0 \leq \varepsilon \leq 0.35$. Values shown here range from 0°, in the isotropic case, to 22° and higher. Figure 3 holds ε constant at 0.15, while letting δ vary; note that the range here is about 6°. Figure 4, by contrast, holds δ constant at 0.05, while letting ε vary; the range here is almost 20°. Figures 2 – 4 all seem to indicate that ε has a more noticeable effect on the maximum deviation than does δ, and that the deviation produced can reach values that are quite large.

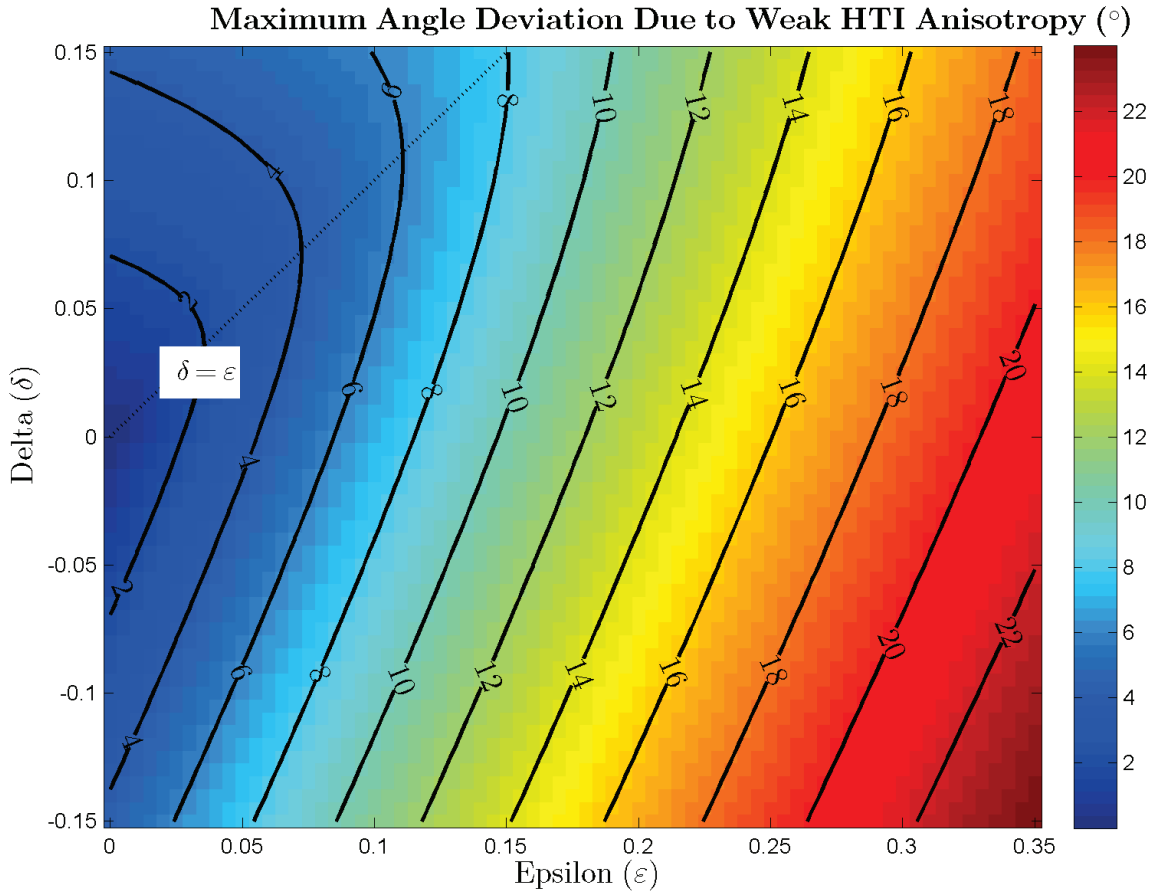

FIG. 2. Maximum difference between group and phase angle, in degrees, as a function of epsilon and delta; the line $\delta = \varepsilon$ is drawn in for convenience.

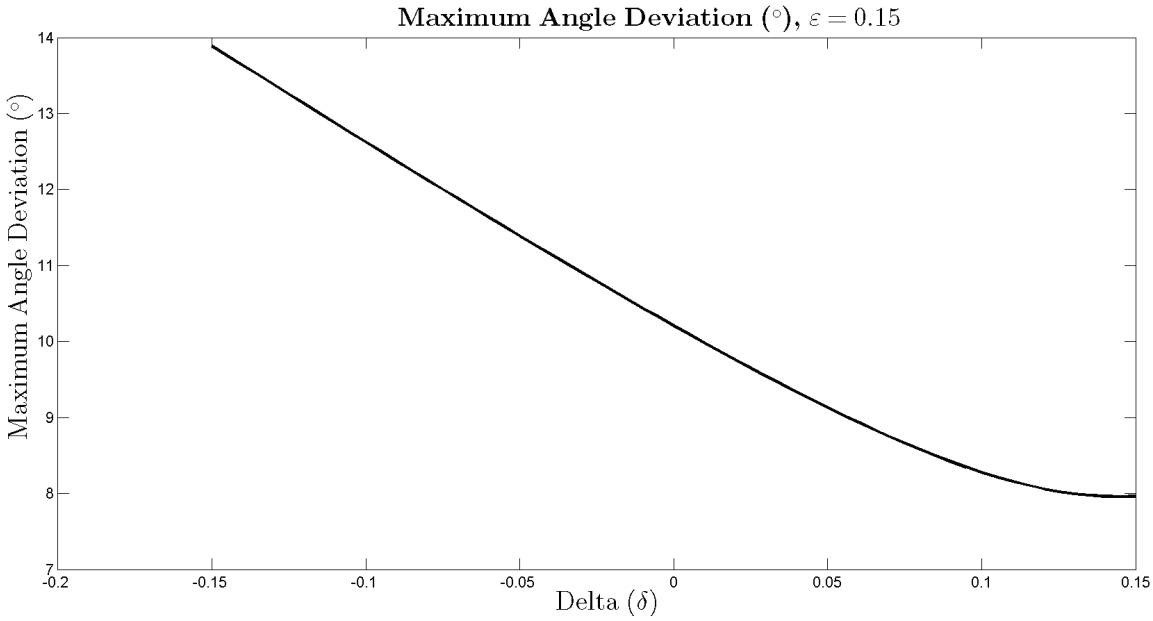

FIG. 3. Maximum difference between group and phase angle, in degrees, using a constant epsilon of 0.15.

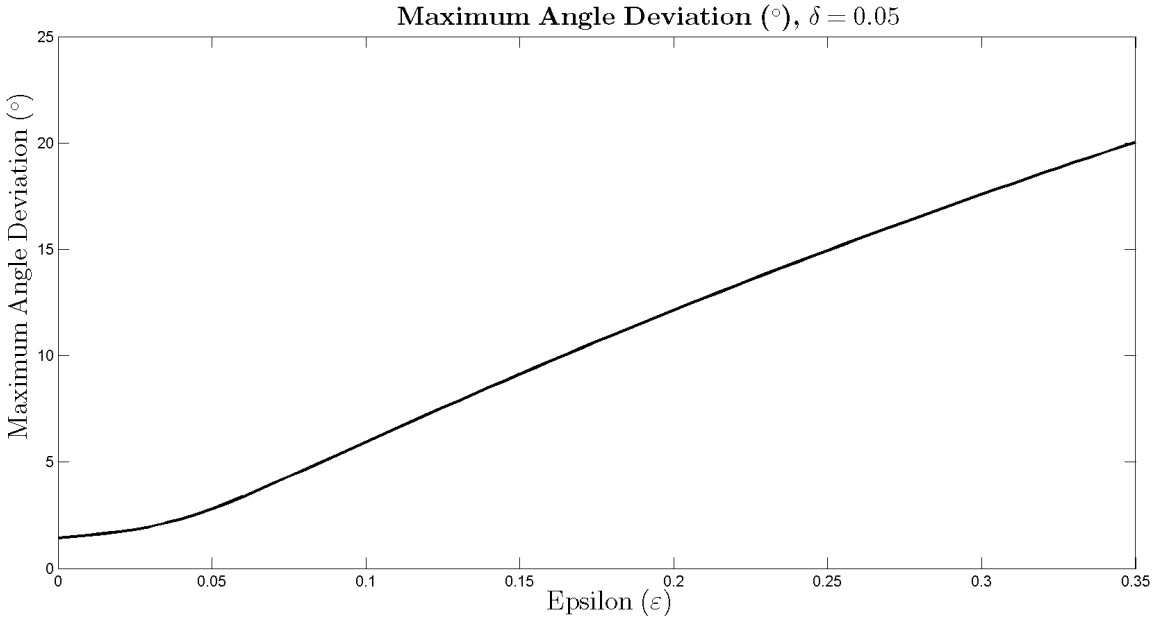

FIG. 4. Maximum difference between group and phase angle, in degrees, using a constant delta of 0.05.

Modelled calibration survey

In order to better understand what the effects of anisotropy will produce in the context of a geophone orientation study, a simple synthetic experiment was devised. The parameters used, taken from results of a Foothills imaging study done by Vestrum et al. (1999), were $\varepsilon = 0.1$ and $\delta = 0.025$. v_0 was chosen to be 3000 m/s, though this choice will not affect the magnitude of angle differences in the case of a single layer. Figure 5 shows the shape of this wavefront as a function of both phase angle and group angle; the differences between them are most noticeable at angles near 90° and 270°. Figure 6 plots the difference between these two angles as a function of phase angle. In this example, the maximum angle difference is 6.45°, which occurs at angles of 57.4°, 122.6°, 237.4° and 302.6°. Note that the angles shown in Figures 5 and 6 are all measured counter clockwise from the positive x-axis (East).

Once the parameters of the medium were chosen, surface geometry was created. Three lines were used in this synthetic experiment: Line 1, trending East-West 200 m north of the well; Line 2, trending north-south 200 m east of the well; and Line 3, intersecting the well at an angle 30° east of north. All three lines had a shot spacing of 100 m, and had a spread of 1500 m in either direction (Figure 7). Finally, the anisotropic axis of symmetry was chosen to be at an azimuth 60° west of north, perpendicular to the azimuth of Line 3. Using these model parameters, the phase angle at each of the shot locations was found; in order to do this, the group angle was first calculated by finding source-receiver azimuth of each location. Next, a table relating group and phase angle was created, to a phase angle precision of 0.1°; this was necessary due to the difficulty of solving Equation 2 directly for phase angle. The table was searched for the closest matching group angle for each shot location, and the matching phase angle found.

Figure 8 shows the difference between the phase and group angles calculated using the modelled survey, as a function of source-receiver offset. In the context of this study, this is effectively the deviation that will be produced for a noise-free geophone orientation calibration. Note that each line follows a distinctly different trend; Line 1 shows predominantly positive deviations, while Line 2 shows predominantly negative deviations. Additionally, the curve produced by Line 2 shows a concave up character for both positive and negative offsets, whereas Line 1 is concave up for negative offsets and concave down for positive offsets. Line 3 shows no deviations; this is an intuitive result, since the azimuth of this line is perpendicular to the symmetry axis. On the other hand, if we examine the orientation angle deviation as a function of source-receiver azimuth, the pattern seen is more consistent between lines (Figure 9). In fact, the relationship appears very similar to that seen in Figure 6, though it is reversed and shifted due to the different angle conventions. Finally, statistical analysis of these values produces a mean value of -0.46°, and a standard deviation of 3.52°.

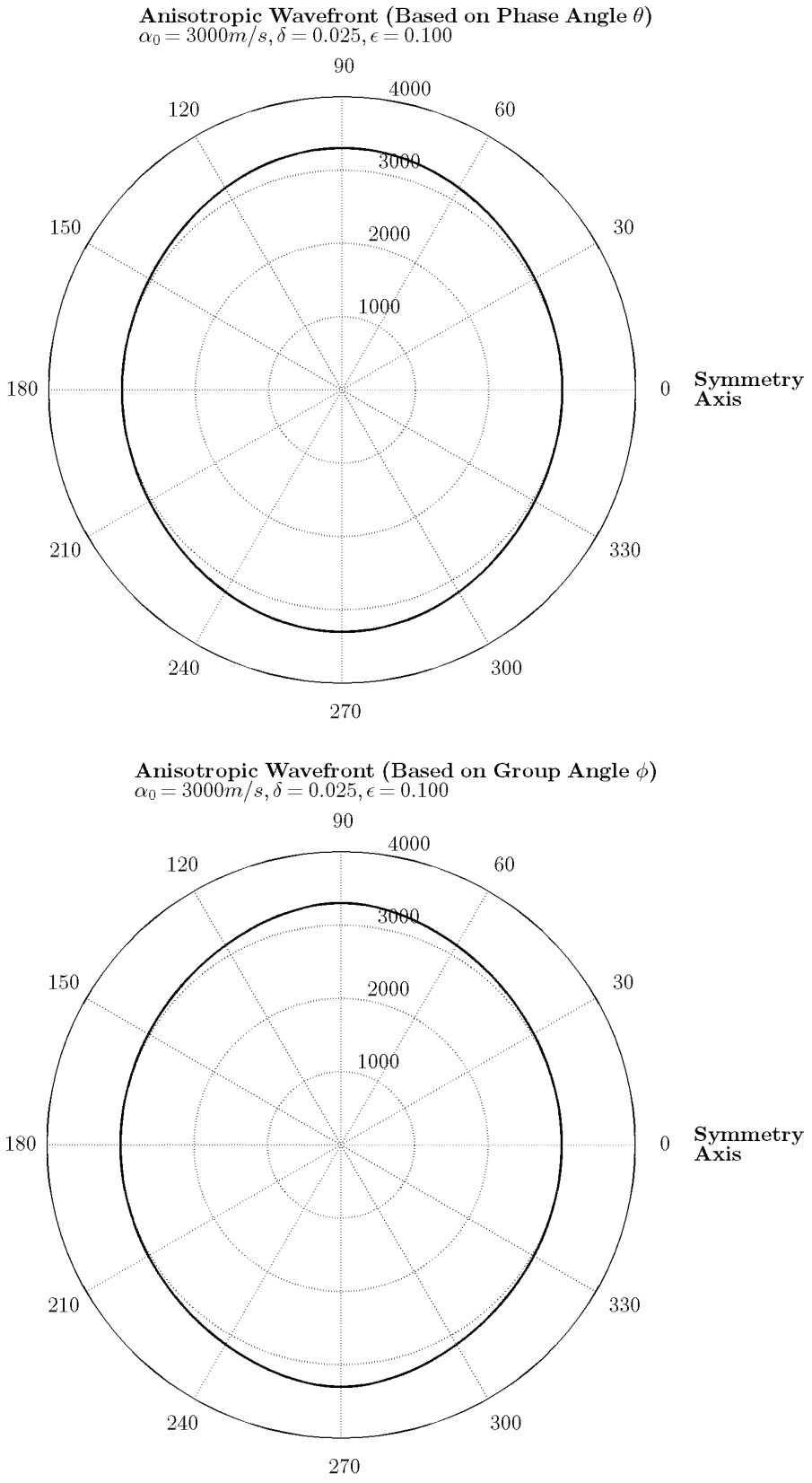

FIG. 5. Anisotropic wavefront as a function of phase angle (top) and group angle (bottom), using parameters v_0 = 3000 m/s, δ = 0.025 and ε = 0.1.

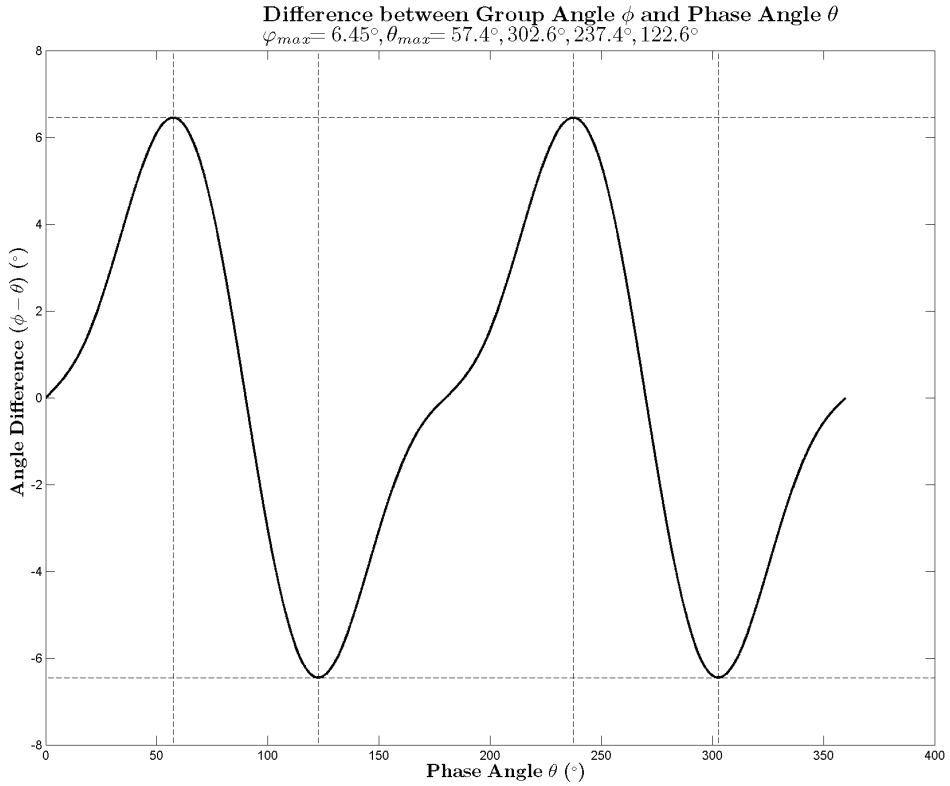

FIG. 6. Difference between group and phase angle, in degrees, using parameters v_0 = 3000 m/s, δ = 0.025 and ε = 0.1.

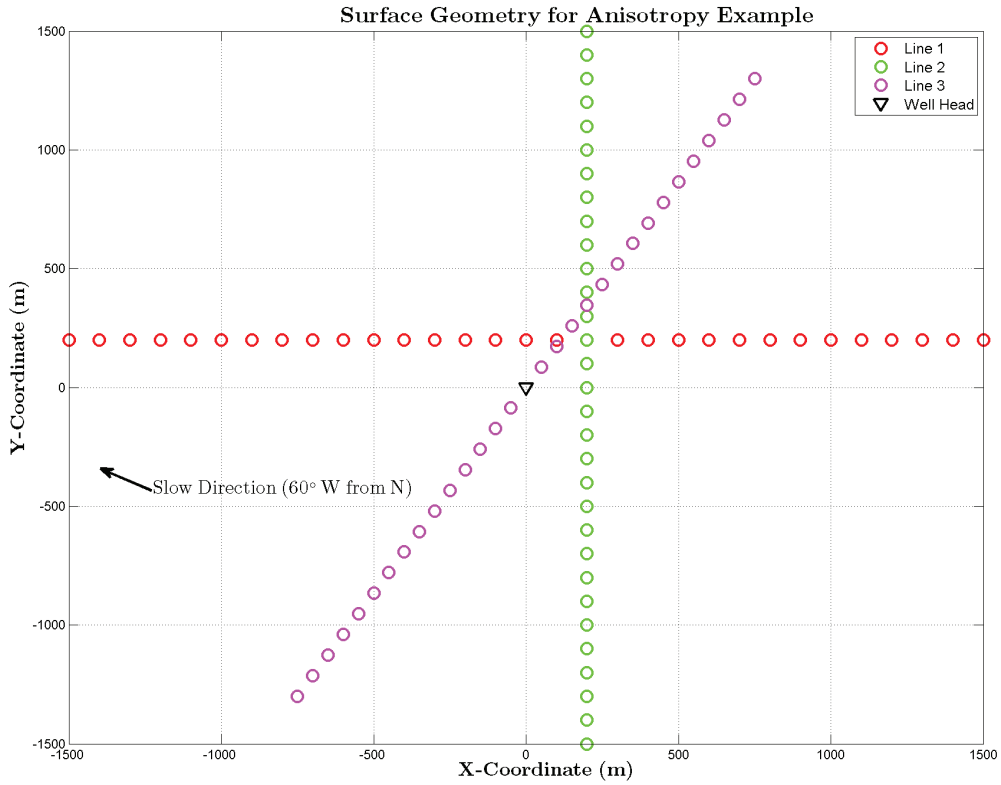

FIG. 7. Surface geometry used in modelled calibration survey.

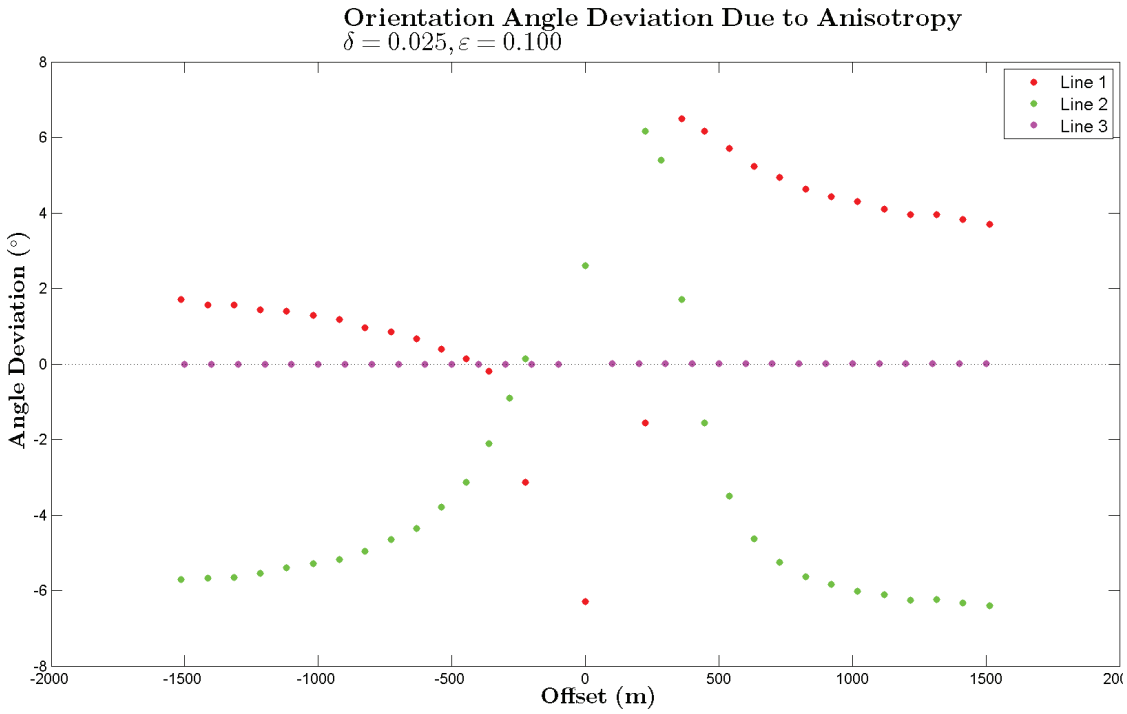

FIG. 8. Calculated deviation in orientation angle due to anisotropy vs. source offset. Deviation for Line 1 is shown in red, deviation for Line 2 is shown in green, and deviation for Line 3 is shown in magenta.

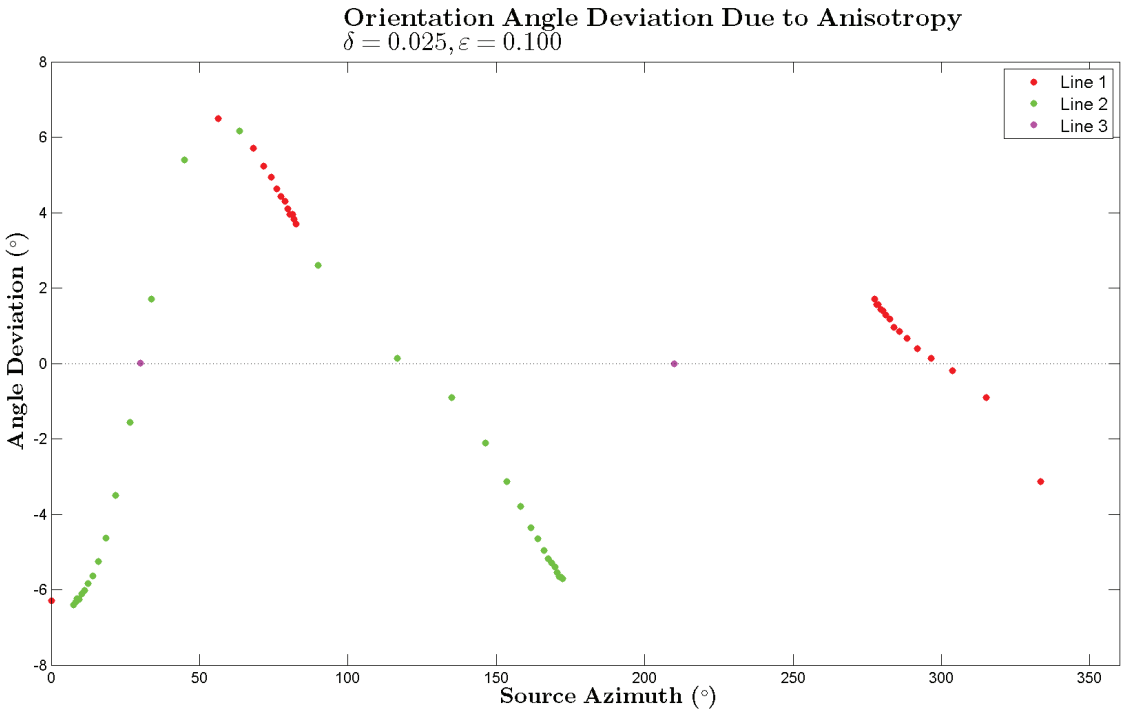

FIG. 9. Calculated deviation in orientation angle due to anisotropy vs. Source-well azimuth. Deviation for Line 1 is shown in red, deviation for Line 2 is shown in green, and deviation for Line 3 is shown in magenta.

DISCUSSION

In the first example presented above, the maximum deviation in angle appears to be more sensitive to ε than it does to δ. At modest values of these parameters, the maximum difference of group and phase angle can exceed 10°; additionally, it was shown to become larger than 5° even with relatively small values for δ and ε. To give a sense of what this means, an error of 5° at 1000 m offset would cause a lateral mispositioning of about 87 m. In a study by Van Dok et al. (2011), the danger of ignoring anisotropy is illustrated by comparing the locations of microseismic events calculated with and without anisotropy considerations; the result is lateral mispositioning of these events by hundreds of feet.

The modelled calibration study also shows some interesting results. First, when plotting the calculated orientation angle deviation against offset, each line shows a distinct, seemingly unrelated trend, making it difficult to interpret the meaning of the results; this is with the exception of Line 3, which was strategically chosen to be parallel to the symmetry axis of the anisotropy, and shows no deviation. The scatter observed in the angles calculated from Lines 1 and 2 may, in fact, be mistakenly attributed to the effects of random noise. However, at the farther offsets, these lines appear to have an asymptotic behaviour; the reason for this is that the source-receiver azimuth is being less affected as the offset increases. This can be seen when examining the plot of orientation angle against source-receiver azimuth – shot locations for Line 1 are approaching azimuths of 90° and 270°, while those for Line 2 are approaching 0° and 180°. This result is encouraging, and suggests that farther offsets will provide a clearer indication that the deviation in orientation angle is due to a geologic effect rather than noise. This parallels the conclusions drawn in previous studies, such as Gagliardi and Lawton (2010, 2011) and Gagliardi et al. (2011), which indicate that the farther offsets in a geophone orientation calibration study have reduced scatter in orientation angle.

CONCLUSIONS

- The maximum deviation in geophone orientation angle due to anisotropy is more sensitive to the parameter ε than it is to δ.
- Even given δ within ± 0.05, deviations in geophone orientation angle can exceed 5° for values of ε as small as 0.05.
- A model created using $\varepsilon = 0.1$ and $\delta = 0.025$ showed a maximum difference in phase and group angle of 6.45°.
- The effect of anisotropy on geophone orientation angle is difficult to interpret when examined as a function of source-receiver offset; however, it produces a much more consistent trend when examined as a function of source-receiver azimuth.
- As the offset increases on a source line, the source-receiver azimuths tend to approach a particular value; this, in turn, means that the deviation in orientation angle due to anisotropy will also approach a particular value.

- Overall, the results of this study show that neglecting anisotropy in geophone orientation calibration analyses can introduce significant error.

FUTURE WORK

The deviations in geophone orientation angle should be modelled in more complex settings, including cases with tilted transverse isotropy, cases with many layers, and cases with dipping beds. A geophone orientation calibration study in an area with known anisotropy would provide further insight into the strength of the anisotropic signature relative to noise content. Finally, the viability to extract anisotropic parameters from geophone orientation information should be considered.

ACKNOWLEDGEMENTS

We would like to thank CREWES sponsors for ongoing support of our research.

REFERENCES

Gagliardi, P. and Lawton, D. C., 2011, Geophone azimuth consistency of a 16-level VSP tool: CREWES Research Report, **23** (this report)

Gagliardi, P. and Lawton, D. C., 2010, Borehole geophone repeatability experiment: CREWES Research Report, **22,** 22.1-22.23.

Gagliardi, P., Innanen, K. A. H. and Lawton, D. C., 2011, Effects of noise on geophone orientation azimuth determination: CREWES Research Report, **23** (this report)

Thomsen, L., 1986, Weak elastic anisotropy: Geophysics, **51,** 1954-1966.

Van Dok, R., Fuller, B., Engelbrecht, L. and Sterling, M., 2011, Seismic anisotropy in microseismic event location analysis: The Leading Edge, **30,** 766-770.

Vestrum, R. W., Lawton, D. C. and Schmid, R., 1999, Imaging structures below dipping TI media: Geophysics, **64,** 1239-1246.